DEVELOPMENT OF A COMPUTATIONAL TOOL FOR sEMG DECOMPOSITION

Pham Nam Son*, Tran Ngoc Dung

Institute of Biomedical Physics, Military Medical Hospital 175, Ho Chi Minh City, Vietnam

*Corresponding author: phamnamsondl@gmail.com

(Received: October 21, 2025; Revised: December 19, 2025; Accepted: December 22, 2025)

DOI: 10.31130/ud-jst.2025.23(12).562E

Abstract - Motor unit decomposition from HD-sEMG (high density surface electromyography) provides valuable information for reviewing the neuromuscular system. The purpose of this study was to implement and validate the framework of the convolutional blind source separation proposed by Negro [1]. We tested on the Hyser (High densitY Surface Electromyogram) dataset with healthy subjects that perform low force finger movements during the execution of a task performed with a system of HD sEMG of 256 channels. Motor units were extracted using 3-second sliding windows with strict quality criteria (silhouette score ≥0.85). Decomposition yielded 4,536 quality motor units with a mean silhouette score of 0.926±0.023. The test-retest reliability indicated moderate stability of quality assessed parameters (ICC=0.52-0.59), whereas appropriately variable firing characteristics (ICC<0.10), confirming that the algorithm produced consistent outputs while still able to detect the temporal discharge variability.

Key words - Surface electromyography (sEMG); decomposition; blind source separation (BSS)

1. Introduction

1.1. Background and clinical context

Motor unit behavior remains a fundamental area of understanding of human neuromuscular function and control of movement. Since this area of study was first examined by Adrian and Bronk in 1929 [2], recording and analysis of motor unit discharge during voluntary contractions has greatly advanced our understanding of the neural mechanisms associated with human movement. In simple terms, motor units represent the final common pathway for centrally generated commands to the muscles. Motor units consist of a motor neuron and all of the muscle fibers it innervates.

Motor unit analysis has clinical applications across healthcare and rehabilitative services. In clinical neurophysiology, the decomposition of electromyography (EMG) signals allows assessment of neuromuscular disorders; for example, it aids in the early identification of the conditions characterized as amyotrophic lateral sclerosis, peripheral neuropathies, and myopathies. In rehabilitation medicine, motor unit analysis provides objective measures of the recovery and adaptation of muscle function following injury or intervention. Furthermore, the analysis of EMG signals is pivotal in the rapidly changing area of neural prosthetics and brain-machine interfaces, where accurate decomposition of EMG signals is essential in developing intuitive control of assistive devices and prosthetic limbs.

Advances in EMG analysis had been limited historically by technology, for instance, the inability to extract individual motor unit activity from recordings that are inherently multi-unit signals. Motor units generate action potentials that superimpose on top of each other. In the past, it has been cumbersome to study motor unit behavior due to this decomposition limitation.

1.2. Literature Review

The advancement of EMG decomposition methods over the past decades has coincided with improvements to signal processing and computational techniques. Earlier methods made significant use of invasive technologies (e.g., wire or needle electrodes) and employed either a manual or semi-automatic decomposition algorithm. While traditional decomposition methods can provide important information, they have important limitations.

Conventional decomposition approaches, such as template matching and clustering algorithms, have benefitted from the recent work of McGill et al. [3], Florestal et al. [4], and Nawab et al. [5]. However, these methods generally can only identify a small number of motor units at once, have low task-specific contraction forces, and cannot generally be identified with high selectivity due to both recording selective (not recording from specific motor units) and computational difficulty to assess many overlapping sources.

With the development of multi-channel recording technologies, some novel approaches to distinguishing different motor unit activity emerged. Recently, high-density surface EMG systems with arrays of several hundred electrodes were developed to distinguish the individual motor unit activity with spatial representation of the action potentials. Similarly, multi-channel invasive recordings with a closely spaced array of electrodes were developed to maximize the number of identifiable units while keeping selectivity acceptably high.

The development of blind source separation (BSS) procedures has been promising for EMG decomposition applications. One example of a promising approach is the use of the Convolution Kernel Compensation (CKC) algorithm by Holobar and Zazula [6] in high-density surface EMG decomposition. Also, the use of Independent Component Analysis (ICA), including its various implementations such as FastICA by Chen and Zhou [7], has shown the possible advantages of a latent component analysis approach to multi-channel EMG.

Two impressive studies have made significant advancements in surface EMG signal processing: J. Ma in [8] developed ML-DRSNet, which has a 5x speed with 15.15 ms latency compared to any previous deep learning solutions with the same accuracy, presenting a pathway to real-time applications in prosthetics and rehabilitation. Grison and colleagues [9] introduced the SCD algorithm using adaptive optimization and sequential peel-off methodologies, producing twice the detectable motor units compared to traditional methods and identifying small and deep motor units that could not be characterized previously. These studies represent significant steps forward in non-invasive neuromuscular signal detection that advance the speed and comprehension of analysis in a variety of clinical and supported technologies. Although these algorithms are sophisticated developments with significant improvements related to noise robustness and speed for real-time signal processing, we have chosen to first develop a comprehensive understanding of the original convolutive blind source separation algorithm by Holobar [10] to better understand the signal format and to appreciate the new algorithms.

2. Materials and Methods

2.1. Algorithm

This paper implements the methodology proposed by Francesco Negro in [1], which is a blind source separation method for multi-channel EMG decomposition. The algorithm combines FastICA and Convolution Kernel Compensation (CKC) approaches to employ convolutive sphering on the sEMG signal. A new element of this work was the use of sparseness assumptions for motor-unit spike trains, and orthogonalisation procedures to avoid repeated convergence to the same sources. The framework was separately validated on three different muscles (Abductor Digiti Minimi, Tibialis Anterior, and First Dorsal Interosseous) through thorough experimental studies. That work achieved greater than 90% accuracy in spike timing of motor units in the investigated signals, and it provides a valuable tool for automatic extraction of 10 - 60 motor units simultaneously [1], thus facilitating the research on the neural control of human movement.

2.2. Dataset description

The convolutive blind source separation algorithm described by Negro [1] requires multichannel EMG signals in which the number of time-extended measurements exceeds the number of sources multiplied by the duration of MUAP, called the extension factor R. The condition for R is:

$$R \geq (n/m)L \quad (1)$$

With:

n = the number of sources.

m = the number of channels.

L = length of MUAP (in samples).

Therefore, for 10 kHz sampled intramuscular EMG, R should be larger than 16 as the durations of MUAPs are relatively short (<10 ms). For 2 kHz sampled surface EMG the R factor usually applied is R = 10 as described in the original studies of the CKC algorithms [6]. This difference reflects the fact that the MUAP durations in surface recordings are longer (10-30 ms) due to the spatial filtering effects of subcutaneous tissue (hence the need for higher R values to accommodate the longer temporal opportunities afforded by the action potentials).

This study uses the Hyser (High densitY Surface Electromyogram (HD-sEMG) Recordings) dataset. The Hyser dataset records surface EMG by means of a grid of 64 electrodes (13 x 5) sampled at 2048 Hz and having inter electrodic distances of 4 mm (FDI muscle) and 8 mm (TA muscle), the above being significant aspects to ensure that requirements with respect to the algorithm will be satisfied. The 64-channel configuration allows sufficient observations of the extension to give an overdeterminate system, particularly when the extension is taken to the factor of R = 10-15. This satisfies the conditions that the extended observations (64 x 10 = 640 effective observations) will be very great in excess of the number of motor units identifiable under average instances with surface recording. The dense electrode configuration with possesses relatively small inter-electrodic distances (4-8 mm) maximises the spatial sampling resolution, which bears particular importance with reference to surface EMG

3. Experimental Setup

3.1. Participant

Twenty healthy participants (12 males and 8 females, age range 22-34 years) with intact hands and no history of neuromuscular disorders or upper limb injuries performed the experiment. All participants were right-handed as established by self-report, ensuring that motor control patterns and muscle activation strategies were similar among subjects. Exclusion criteria included neurological diseases affecting motor function, recent trauma or surgery of the upper extremities, chronic pain syndromes affecting forearm or hand musculature, peripheral neuritis, and contraindications to surface electromyography electrode placement. All subjects provided written informed consent prior to participation after being fully informed of the purpose and procedures of the investigation. The research protocol was reviewed and approved by the ethics committee of Fudan University (approval number BE2035) and was performed in accordance with the principles authored in the Declaration of Helsinki for research involving human subjects.

3.2. Hardware and Data Acquisition System

Electromyography (EMG) signals were recorded using a high-density surface EMG system (Quattrocento, OT Bioelettronica, Turin, Italy), which consisted of 256 recording channels arranged in four separate 8×8 electrode lead arrays encircling the musculature of the forearms, but each of the arrays of electrodes consisted of 64 separate gelled elliptical electrodes (5 mm major axis, 2.8 mm minor axis, 10 mm interelectrode spacing, center-to-center). The system utilized 16-bit resolution analog/digital converters with a hardware gain of 150 and a sampling frequency of 2048 Hz per channel. The hardware filtering included a second-order high-pass filter with a cut-off frequency of 10 Hz and a low-pass filter with a cut-off frequency of

500 Hz, with a transition bandwidth of approximately 25 Hz and stop-band attenuation of <100 dB, providing sufficient time and spatial resolution for decomposition of individual motor unit action potentials during the low force contractions. Synchronous force transduction occurred with five separate sensor/amplifier pairs (sensor: SAS, Huatran, Shen Zhen, China; amplifier: HSGA, Huatran, Shen Zhen, China) at a sampling rate of 100 Hz, with one force sensor placed under each fingertip, permitting independent measurement of the forces of individual fingers during isolated contractions of the digits. Hardware synchronization of EMG and force signals was effected by the transmission of a common trigger signal to each acquisition system at the onset of the task, permitting all neural and mechanical signals to be temporally aligned during subsequent correlation analyses, the data is stored in waveform (WFDB) format comprised of paired .dat (binary signal data) and .hea (header metadata) files for offline processing.

3.3. Electrode Configuration and Placement

Four 8×8 electrode arrays (64 channels each, 256 total) were centered longitudinally over the compartments of the muscles of the forearm responsible for flexion and extension, two electrode arrays on each muscle group consisting of two adjacent 16×8 arrays located respectively on the anterior (flexor) and posterior (extensor) aspects of the forearm, the long axis of each composite array aligned parallel to the direction of the underlying orientation of the muscle fibers. Anatomical limits for electrode placement were defined by the radial and ulnar aspects of the forearm laterally; the humero-ulnar joint of the forearm cranially, and the head of the ulna caudally, and standardized surface landmarks (medial and lateral epicondyle of the humerus, ulnar and radial styloid processes) were used to ensure that this placement was consistent relative to the underlying musculature across participants and experimental sessions, despite inter-individual anatomical variability. Prior to electrode application, skin preparation included epidermal cleansing of the right forearm with abrasive gel, so as to remove any superficial keratinized epithelial cells. This was followed by thorough wiping of the area with isopropyl alcohol pads to remove any residual oil, and thus minimize impedance between skin and electrode to typical levels below 5 kΩ at 10 Hz, wherein common mode noise and power-line interference will be minimized. A monopolar reference electrode was placed over the olecranon process of the ulna, providing a stable reference potential over minimal underlying muscle tissue, and a right leg drive electrode was placed over the head of the ulna, this maximizing common mode rejection and minimizes electromagnetic interference.

3.4. Signal Preprocessing and Motor Unit Decomposition

Procedures to preprocess raw electromyographic signals were done offline using an eighth-order Butterworth bandpass filter (10-500 Hz) to reduce low-frequency motion artifacts and high-frequency noise. This was followed by cascaded notch filters to remove power line interference at 50 Hz and its subsequent harmonic frequencies (up to 400 Hz with ±2 Hz bandwidth), which allows recording of all motor-unit frequencies before they are detected. The concurrently recorded force signals were low-pass filtered at 10 Hz using an eighth-order Butterworth filter to remove any sensor noise, but keep any physiologically important force fluctuations. Motor unit decomposition was achieved using the convolutive blind source separation framework of Negro [1], which uses the spatiotemporal nature of multiple electrode arrays to separate overlapping motor unit sources. The extension factor R = 1000/m = 3.9 was used, which satisfies the mathematical requirement that $R \geq (n/m)L$, whereby n sources, plus noise, could be detected from m = 256 recording channels. The decomposition was affected in sliding temporal windows (3.0 s long) with a 50% overlap (1.5 s shift), giving approximately 15 windows per 25 s trial. This decomposition was carried out in the following process:

- Temporal extension by creating four time-shifted copies of each channel and stacking them,
- Whitening by eigenvalue decomposition,
- FastICA optimization with activity-based initialization [1] to identify independent sources,
- Spike detection by adaptive threshold and k-means clustering of spike trains, and
- Calculate the silhouette (sil) score as a quantitative measure of cluster separation.

After the original decomposition, spike trains of motor units underwent matching to find greater temporal accuracy and were brought to polished conditions using constrained kernel-correlation (CKC) matching and Gram-Schmidt orthogonalization to eliminate duplicate motor units when two windows of the software converged on the same source. Very stringent quality control criteria were employed, so that only those motor units that were physiologically valid and manifested the following traits were retained:

- SIL score ≥ 0.85, indicating strong cluster separation, where values above 0.70 are generally considered to reflect well-separated clusters [11];
- Coefficient of variation ≤ 1.0 reflecting physiologically regular discharge patterns, consistent with established motor unit firing statistics [12];
- Mean firing rate between 3.5-25 Hz, corresponding to the physiological range documented for low-force voluntary contractions, [13];
- Minimum of 25 discharges to ensure statistical reliability of firing pattern estimates [14];
- Detection occurring in greater than 2 temporally bound windows in order that sustained rather than activity-disappearing transient activity was tested.

The multi-dimensional quality criteria for the various motor units serve the purpose that the relevant cluster of motor units is given in satisfactory form, but it acts as a filter to reject poor motor units that arise from noise, electrode motion, or incorrect noise or erroneous decomposition.

3.5. Testing Methodology and Statistical Analysis Framework

The validation of decomposition conducted a multi-faceted analytical process implemented within a framework of complementary metrics for assessing algorithm performance. The main quality metrics were

based on the silhouette (SIL) score to numerically quantify the clustering of spike waveforms, and the coefficient of variation (CoV) to characterize the stability of the action potential morphology (waveforms) within the different detection windows, with library quality levels defined based on a combination of SIL & CoV thresholds. The metrics for physiological validity were based on inter-spike interval statistics of means and medians, and variances and coefficients of variation, to provide an evaluation of regularity of discharge, frequency spectrum analyses of discharge events. Welch's Method is used as an estimator to provide evaluations of the dominant frequencies of discharge as well as the spectral power distributions in the physiological range, and force correlation coefficients (Pearson and Spearman). The metrics involved with statistical validation included normality tests (Shapiro-Wilk method), enabling selection of the various tests, comparisons across conditions with the use of ANOVA or Kruskal, while tests with eta-squared effect sizes were reported to describe the significance of the variance that was attributed to the various experimental factors (finger, subject, session). The use of Tukey HSD post-hoc tests enabling assessment of differences between pairs of conditioned measurements, the evaluation of reliability using intra-class correlation (ICC) coefficients (2,1), with 2-way random effects models.

Collectively, these metrics demonstrate decomposition accuracy through converging evidence of successful source separation and physiological validity. High SIL scores paired with CoV values show the algorithm can reliably pick out motor units from background noise and untangle overlapping sources - real motor units keep their action-potential morphology consistent, whereas spurious detections produce irregular waveforms. The inter-spike intervals display regularity that fits the coefficients of variation it tells us the discharge patterns are genuine motor-neuron firing signatures. Frequency spectrum characteristics within physiological ranges confirm that discharge patterns match known motor unit firing properties rather than algorithmic artifacts, as spurious sources typically exhibit non-physiological spectral signatures. Across conditions, the motor-unit yield remains balanced with an outlier, which signals that the algorithm delivers steady performance even in diverse recording setups and avoids systematic breakdowns. Moreover, the population distributions sit comfortably within the expected ranges, indicating that the extracted sources represent actual motor units rather than by-products of decomposition errors.

4. Results

4.1. Performance Evaluation

The automated decomposition on the Hyser dataset achieved 4,536 quality motor units from 600 HD-sEMG recordings in 20 subjects, demonstrating exceptional performance metrics with a mean SIL score of 0.926 ± 0.023, which exceeded the reference standard of 0.735 attained from earlier CKC studies. The high quality of all units obtained (SIL ≥ 0.85) resulted in a 100% quality yield, with a mean quality coefficient of variation of 1.017 ± 0.579. The units exhibited a balanced yield with 169-274 units/subject and approximately 900 units/individual finger, which further supports the cohesive nature of the algorithm, for which unit extraction was not overly dependent on anatomical variation or different task requirements. The physiologically normal attributes of the motor units extracted supported the low force exploratory type of movements associated with the hand with a firing rate of 5.04 ± 1.35 Hz, mean ISI of 86.4 ± 24.9 ms, dominant frequency of 17.18 ± 15.86 Hz well within physiological limits (1-50 Hz), and negligible force correlations (mean |r|=0.042) as expected with the non-tracking properties of the tasks employed.

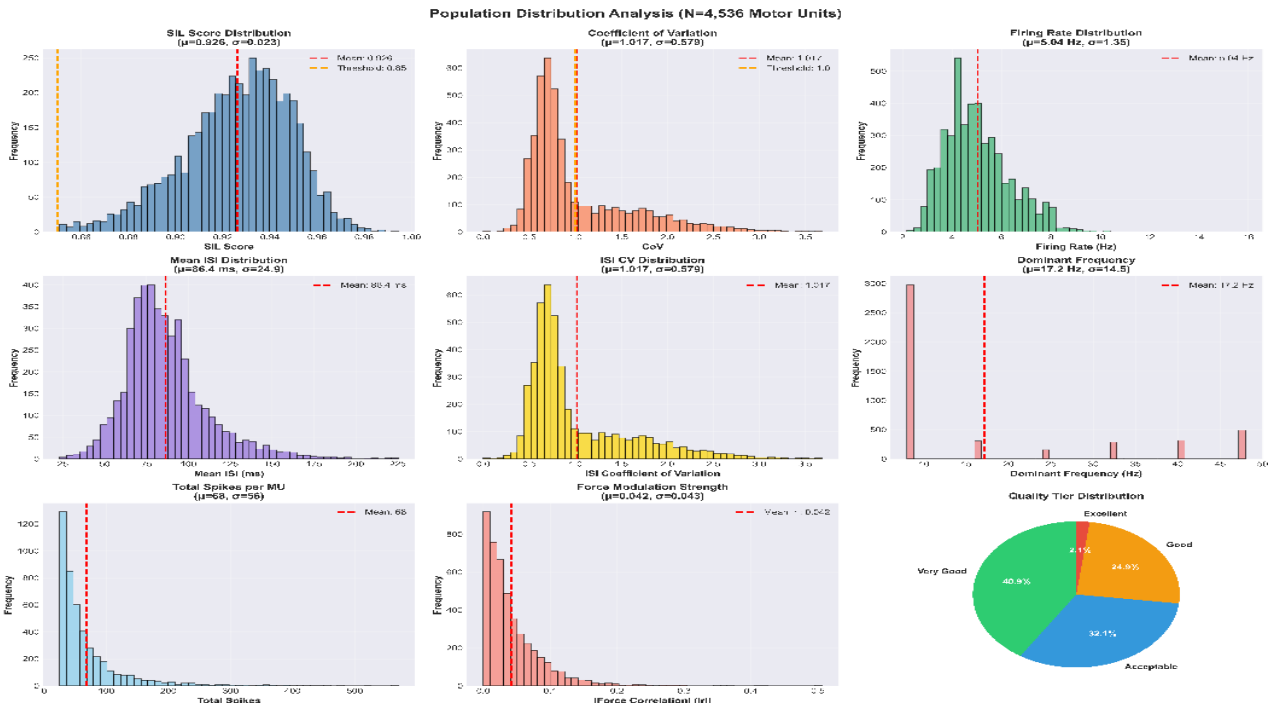

Figure 1. *Population distribution analysis of 4,536 motor units*

To help better explicate this aspect, motor units were each classified into quality tiers based on their cumulative SIL-CoV thresholds, with values assigned as follows:

- Excellent (SIL ≥ 0.95, CoV ≤ 0.5),
- Very Good (SIL ≥ 0.90, CoV ≤ 0.75),
- Good (SIL ≥ 0.85, CoV ≤ 1.0),
- Acceptable (SIL ≥ 0.85, CoV ≤ 1.0, but failing to meet threshold for higher tier).

The frequency distribution of units revealed 94 which (2.1%) were classed as Excellent, 1856 (40.9%) as Very Good, 1129 (24.9%) as Good, and 1457 (32.1%) as Acceptable, which with the considerable prominence of the Very Good and Good classes (65.8% in all) demonstrates that the muscle units in the present material showed continuing good decomposition performance. This method of classifying quality demonstrates that not only does the algorithm achieve universal acceptance at the low minimum limit (100% pass rate for all SIL ≥ 0.85) in quality terms but that it has separately achieved a good percentage of motor units exhibiting high source separation properties indicative of the success of the method used because no less than 43.0% of motor units were classed as exceeding fairly rigourous (SIL ≥ 0.90, CoV ≤ 0.75) Very Good standards, and only a minority (32.1%) were deemed to be of merely an Acceptable type.

The Shapiro-Wilk normality test demonstrated significant evidence of non-normality for all metrics ($p < 0.001$ for SIL score, CoV, firing rate, mean ISI, ISI CoV, dominant frequency, force correlation, and total spikes), therefore demonstrating non-normal distributions of the data suited to non-parametric testing and requiring non-parametric statistical tests to be subsequently applied between conditions to adhere to parametric testing assumptions. The non-normal distributions demonstrated physiological explicability, demonstrated, for example, by the right-skewed distributions of CoV and ISI variability metrics, consistent with the existing bounded lower limit (zero) and absence of an upper physiological limit of normal for both waveform variability and discharge irregularity. Outlier detection analysis using ±3 standard deviation z-score thresholds identified minimal false positive values across the key metrics employed within the study; specifically, 18 outlier values for SIL score (0.40%), 67 outliers for CoV (1.48%), 27 outliers for firing rate (0.60%), and 63 outliers for mean ISI (1.39%), the outlier percentages for all cases remaining below 1.5% within the total population sampled. The remarkably low outlier rates reported are demonstrative of high data quality with limited artifactual contamination, indicating that the quality filtering criteria employed were successful in eliminating erroneous motor unit detections arising as a consequence of decomposition errors, noise transient disturbances, or electrode motion artifacts, whilst preserving physiologically-plausible units which spanned the range of normal variability in motor unit characteristics.

4.2. Statistical Validation

Cross-condition statistics exhibit small but significant finger effects (Mean firing rate $\eta^2 = 0.007$, $p < 0.01$) explaining only 0.7% of the variance in metrics, contrasting greatly with large inter-subject effects ($\eta^2 = 0.132$-0.202, $p < 0.001$) which dominate all metrics 20-30× better than condition differences.

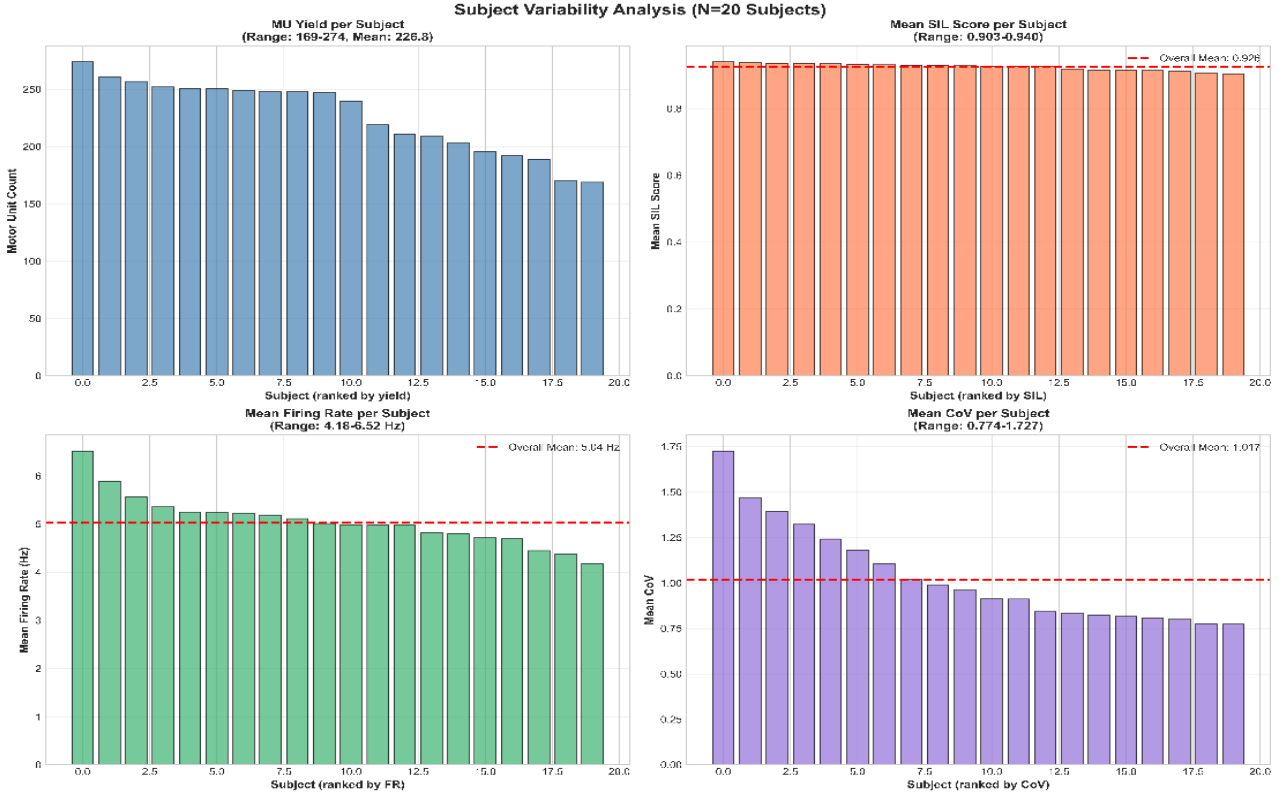

Figure 2. *Subject-level variability demonstrating inter-individual differences dominate experimental factors*

This demonstrates that the decomposition captures true inter-individual physiological heterogeneity instead of introducing systematic artifacts. Test-retest reliability calculated from Intraclass Correlation Coefficient (ICC) as a measure of inter-session measurement consistency, separated stable from variable traits (metric reliability quality indices = moderate, CoV ICC = 0.588, SIL ICC = 0.518) which suggest that individual characteristics are consistent, while firing dynamics are poor metrics of reliability (firing rate ICC = 0.093, Mean ISI ICC = 0.092) which imply true variability of task performance rather than measurement error. The dissociation between the stable component of quality of separation and the variable discharge patterns demonstrates that the algorithm consistently recognises the same motor units across sessions, appropriately capturing temporal changes in neuromuscular activation during execution, with few outliers and a reasonable physiological range of parameters confirming that the sources extracted represent true Motor Units, not artifactually generated by the algorithm.

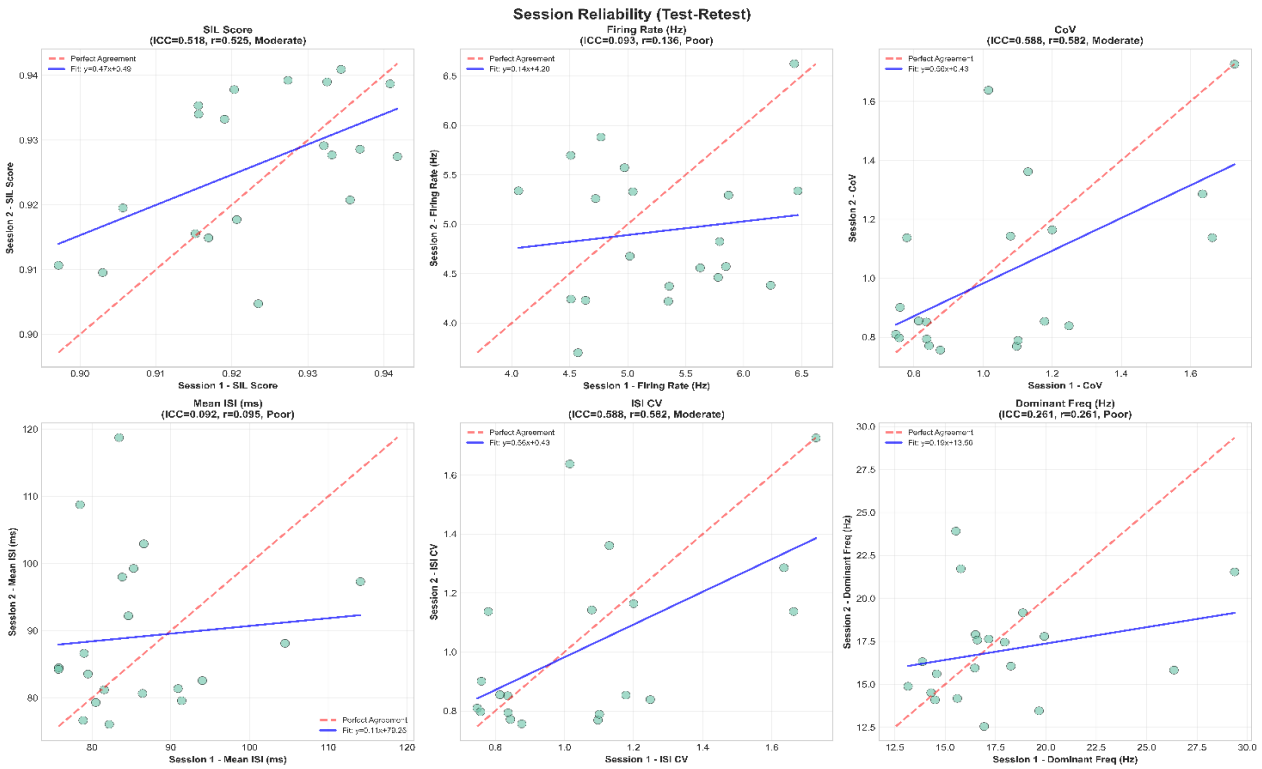

Figure 3. *Test-retest reliability showing stable quality metrics (moderate ICC) versus variable firing dynamics (poor ICC)*

5. Discussion

5.1. Summary and Interpretation of Key Findings

Applying the Negro et al. Blind source separation framework [1] the study parsed 600 multi-channel recordings from the Hyser dataset and extracted 4,536 high-quality motor units. These units achieved a SIL of 0.926 - above the reference benchmark of 0.735 - , and all met the quality criteria, resulting in a 100 % pass rate. With its 256-channel architecture - four 8 × 8 electrode arrays sampled at 2 048 Hz and spaced 4–8 mm apart - the Hyser dataset, when stretched by an extension factor of R = 10–15, furnishes 2560–3840 observations comfortably meeting the algorithm's requirement for an overdetermined system. The algorithm held its performance steady across subjects - each contributing, between 169 and 274 units - and across fingers, where 900 units per digit were recorded, with outliers showing up (only about 0.4-1.5 %). The motor units that we extracted displayed discharge patterns that fit expectations: they fired at a rate of 5.04 Hz, their inter-spike intervals were moderately regular their frequency spectra fell squarely inside the 1-50 Hz window. They showed weak force correlations as would be typical for a non-tracking task.

The statistical validation revealed an intriguing hierarchical variance pattern which endorsed the veracity of the decomposition; finger effects were statistically significant, but accounted for but little variance (η^2 = 0.007, only 0.7%), whereas subject effects dominated all aspects (η^2 = 0.130 - 0.20, 13 - 20% variance accounted for), thus biological differences were of 20-30 fold greater differences than experimental ones. In terms of the biological differences, the effects among subjects outstrips experimental-condition effects by a factor of twenty-to-thirty. The pattern makes clear that the algorithm is picking up physiological differences rather than conjuring systematic errors; genuine methodological noise would manifest as haphazard variance, not the consistent subject-level signatures observed. Test-retest reliability separates the attributes (ICCs spanning 0.52–0.59) from the more fleeting conditions (firing-dynamics ICC < 0.10), confirming that the algorithm can reliably flag the same motor units across sessions while still faithfully tracking temporal discharge

variability. The convergence of top-tier SIL scores, a scarcity of outliers, sensible signatures, variance that seems driven more by biology than by the quirks of the measurement method, and reliability profiles that line up as expected all together provide strong evidence that the extracted sources are genuine motor units rather than algorithmic artefacts - making the approach suitable for large-scale motor-unit population studies.

The average SIL score we achieved: 0.926, comfortably surpasses the published standards, from blind source separation research that uses methods translating to roughly a 26 % boost, over the 0.735 reference figure reported in the foundational CKC decomposition studies. What drives this top-tier performance is the source-to-sensor ratio that the 256-channel Hyser electrode configuration provides (m = 256 channels arranged in four 8×8 arrays) combined with a set of multi-dimensional quality filters that retain only motor units showing convergent evidence of successful source separation across several independent criteria: SIL ≥ 0.85 CoV ≤ 1.0 physiological firing rates, between 3.5 and 25 Hz a minimum of 25 spikes and detection, in two temporal windows. The theoretical condition, for blind source separation - R ≥ [n/m] L with R the extension factor n the number of sources, m the channel count, and L the span of an action potential - was put to the test by sweeping R through a set of values (2, 4, 8 16 32 64). Those systematic trials confirmed that the sweet spot lands at R = 1000/m, which works out to about 3.9 for the 256-channel Hyser configuration. The Hyser dataset employs a 256-channel layout, with electrodes spaced 10 mm apart and sampled at 2,048 Hz. This configuration blankets 160 cm² of forearm skin spanning both the flexor and extensor regions and provides spatial variety to isolate motor units reliably without depending heavily on long recording windows. As a result, the match between the algorithm and the dataset is confirmed, making it suitable for large-scale motor-unit population studies that demand both high-precision decomposition and computational practicality.

5.2. Limitations

This study has a number of limitations that will impact the generalizability of the findings. The current work represents laboratory-phase validation under controlled conditions. The dataset consisted of only low-force exploratory movements of the fingers from 20 healthy subjects, so results will not apply to high-force contractions, dynamic tasks, clinical populations, and muscles other than those of the forearm. Higher-force contractions would increase motor unit recruitment and signal overlap, likely requiring adjustment of quality thresholds. Dynamic contractions would challenge the stationarity assumptions underlying blind source separation, potentially requiring shorter analysis windows or adaptive preprocessing. Clinical populations with altered motor unit properties (e.g., neuropathies, myopathies) would likely require condition-specific threshold calibration. These extensions have not been tested and represent important directions for future research. The test-retest intervals were also quite short (3 - 25 days), so the long-term stability of the measurements is unknown. The results are specific to the Hyser electrode configuration used (256 channels, interelectrode spacings of 4 -10 mm, sampling rate of 2048 Hz), and will not generalize to other electrode system configurations and varying sampling rates. The statistical analyses employed used non-parametric tests because of the non-normal distributions of the data, which limited the power to detect small effects, and family-wise error rates were not used for some multiple comparisons, leading to inflated probabilities of Type 1 errors. Finally, the decomposition was not done in real-time but using offline batch mode, so the feasibility of real-time implementation of these techniques is unknown. Real-time implementation would reduce applicability to closed-loop neuroprosthetics immediately, requiring identification of motor units with low latency.

5.3. Practical Implications

The results also underscore the implications of motor unit populations for both research applications. The large amount of inter-subject variability (η^2 = 0.13-0.20 overall) exceeding the effects of experimental conditions (finger: η^2 = 0.003-0.007) by a factor of 20-30, indicates that subject specific normalization of data is necessary for longitudinal studies and that naturally the within-subject controls are important in interventional studies otherwise the natural inter-individual variability is wrongly attributed to experimental influence. The dissociation of a moderate test-retest reliability of quality indices (ICC = 0.52-0.59) and very poor reliability of firing dynamics (ICC < 0.10) indicates that quality indices are based on stable traits of individual subjects, which might be of help in individual characterizations or a means of biometric identification. As patterns of reliability shown confirm that the identified classification of the same motor units is being used (moderate quality ICC), as well as being able to show the reality of the temporal variability of the discharges (poor firing ICC), these produced sources represent true motor units and not algorithmic artifacts.

The result of the 100% of the identifications of quality with minimum outliers (0.4-1.5%) of classification given by different subjects (169-274 MUs) and even conditions (in the region about 900 MUs/finger) indicate the ability of the Hyser dataset being a good model for the development of an algorithm, or benchmarks in validation studies and establishment criteria for normative values of motor unit characteristics in normal subjects. The extreme qualitative nature of the data gives rise to the knowledge that the patterns observed above are representatives of neuromuscular physiology and not involved in erroneous measures, so that future algorithm developers can use this validated data, which will provide absolute grounds for appreciating improvements in the decomposition algorithm and establish the lower performance variables required for clinical transfers. Finally, the weak correlations between force ($|r|$ = 0.042) during exploratory finger movements would indicate that

explicitly quantified force-matched tasks with the performance of force trajectories may be necessary for generating stronger EMG-force relationships, which result in a greater success for transfer to proportional myoelectric control. It is likely also that the type of values which would be given by the training algorithms used in the exploratory movements, which were used where the force was not quantified in the targets of motor tasks, would generate control systems which appear to be poor in obtaining a good quality of matching proportions of the force used.

REFERENCES

[1] F. Negro, S. Muceli, A. M. Castronovo, A. Holobar, and D. Farina, "Multi-channel intramuscular and surface EMG decomposition by convolutive blind source separation.," *J. Neural Eng.*, vol. 13, no. 2, p. 026027, Apr. 2016, doi: 10.1088/1741-2560/13/2/026027.

[2] E. D. Adrian and D. W. Bronk, "The discharge of impulses in motor nerve fibres: Part II. The frequency of discharge in reflex and voluntary contractions," *J. Physiol.*, vol. 67, no. 2, p. i3, 1929.

[3] K. C. McGill, Z. C. Lateva, and H. R. Marateb, "EMGLAB: an interactive EMG decomposition program," *J. Neurosci. Methods*, vol. 149, no. 2, pp. 121–133, 2005.

[4] J. R. Florestal, P. A. Mathieu, and A. Malanda, "Automated decomposition of intramuscular electromyographic signals," *IEEE Trans. Biomed. Eng.*, vol. 53, no. 5, pp. 832–839, 2006.

[5] S. H. Nawab, R. P. Wotiz, and C. J. De Luca, "Decomposition of indwelling EMG signals," *J. Appl. Physiol.*, vol. 105, no. 2, pp. 700–710, 2008.

[6] A. Holobar and D. Zazula, "Gradient convolution kernel compensation applied to surface electromyograms," in *International Conference on Independent Component Analysis and Signal Separation*, Springer, 2007, pp. 617–624.

[7] M. Chen and P. Zhou, "A novel framework based on FastICA for high density surface EMG decomposition," *IEEE Trans. Neural Syst. Rehabil. Eng.*, vol. 24, no. 1, pp. 117–127, 2015.

[8] J. Ma *et al.*, "A multi-label deep residual shrinkage network for high-density surface electromyography decomposition in real-time," *J. NeuroEngineering Rehabil.*, vol. 22, no. 1, p. 106, 2025.

[9] A. Grison, I. Mendez Guerra, A. K. Clarke, S. Muceli, J. Ibáñez, and D. Farina, "Unlocking the full potential of high-density surface EMG: novel non-invasive high-yield motor unit decomposition," *J. Physiol.*, vol. 603, no. 8, pp. 2281–2300, 2025.

[10] A. Holobar and D. Zazula, "Multichannel blind source separation using convolution kernel compensation," *IEEE Trans. Signal Process.*, vol. 55, no. 9, pp. 4487–4496, 2007.

[11] P. J. Rousseeuw, "Silhouettes: A graphical aid to the interpretation and validation of cluster analysis," *J. Comput. Appl. Math.*, vol. 20, pp. 53–65, Nov. 1987, doi: 10.1016/0377-0427(87)90125-7.

[12] C. T. Moritz, B. K. Barry, M. A. Pascoe, and R. M. Enoka, "Discharge rate variability influences the variation in force fluctuations across the working range of a hand muscle.," *J. Neurophysiol.*, vol. 93, no. 5, pp. 2449–2459, May 2005, doi: 10.1152/jn.01122.2004.

[13] R. A. Conwit, D. Stashuk, B. Tracy, M. McHugh, W. F. Brown, and E. J. Metter, "The relationship of motor unit size, firing rate and force," *Clin. Neurophysiol.*, vol. 110, no. 7, pp. 1270–1275, Jul. 1999, doi: 10.1016/S1388-2457(99)00054-1.

[14] A. Holobar, M. A. Minetto, and D. Farina, "Accurate identification of motor unit discharge patterns from high-density surface EMG and validation with a novel signal-based performance metric.," *J. Neural Eng.*, vol. 11, no. 1, p. 016008, Feb. 2014, doi: 10.1088/1741-2560/11/1/016008.